AD-A119 184 STANFORD UNIV CA F/G 20/5
RESULTS OF THE FIRST PHASE OF THE ACO STORAGE RING LASER EXPERI--ETC(U)
JUN 81 C BAZIN, M BILLARDON, D A DEACON F49620-80-C-0068
UNCLASSIFIED AFOSR-TR-82-0696 NL

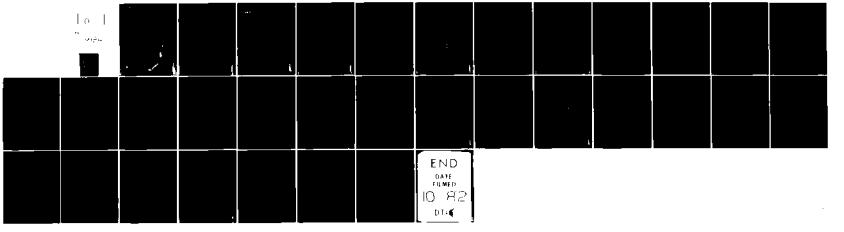

END
DATE FILMED
10 82
DTIC

Centre National de la Recherche Scientifique
Université Paris-Sud

Laboratoire pour l'Utilisation du Rayonnement Electromagnétique

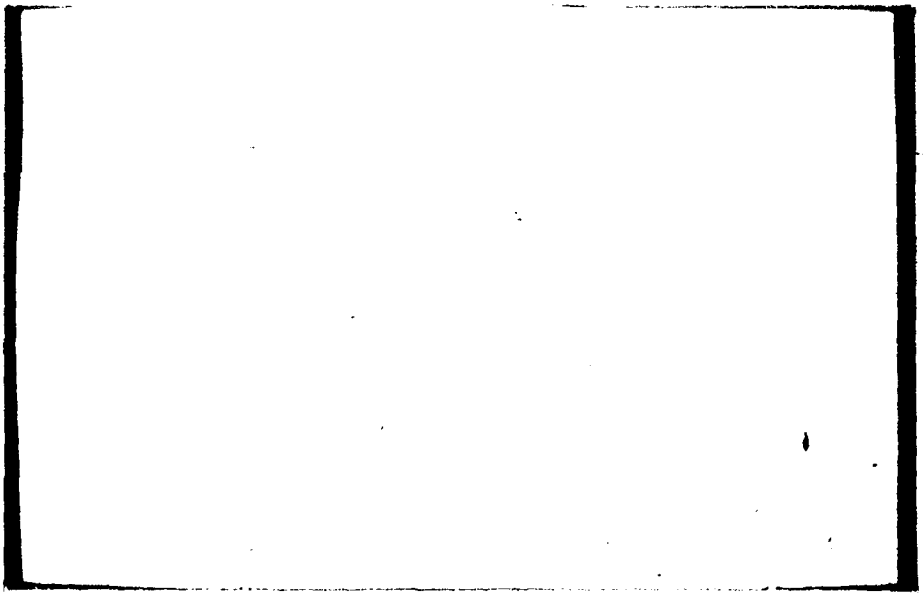

L.U.R.E.
BATIMENT 209 C
UNIVERSITE PARIS-SUD
91405 ORSAY CEDEX
FRANCE

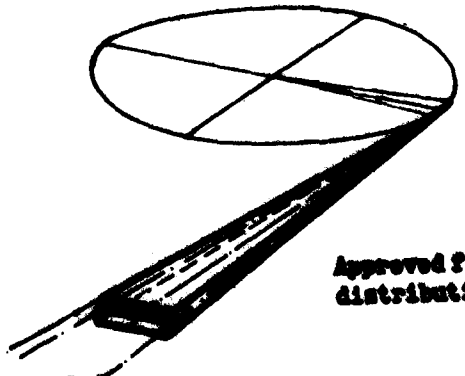

June 1981

RESULTS OF THE FIRST PHASE OF THE A.C.O. STORAGE RING LASER EXPERIMENT

C. Bazin, M. Billardon, D.A.G. Deacon, P. Elleaume, Y. Farge, J.M.J. Madey, J.M. Ortéga, Y. Pétroff, K.E. Robinson, M. Velghe.

Presented at the 1981 ONR Workshop on Free Electron Laser (Sun Valley)

to be published in :

Physics of Quantum Electronics, 8-9 (Addison-Wesley, 1982) eds. Jacobs, Moore, Pilloff, Sargent III, Scully and Spitzer.

UNCLASSIFIED

SECURITY CLASSIFICATION OF THIS PAGE (When Date Entered)

REPORT DOCUMENTATION PAGE	READ INSTRUCTIONS BEFORE COMPLETING FORM
1. AFOSR-TR- 82-0696	2. GOVT ACCESSION NO. AD-A119184	3. RECIPIENT'S CATALOG NUMBER
4. TITLE (and Subtitle) RESULTS OF THE FIRST PHASE OF THE A.C.O. STORAGE RING LASER EXPERIMENT	5. TYPE OF REPORT & PERIOD COVERED INTERIM 6. PERFORMING ORG. REPORT NUMBER
7. AUTHOR(s) C. BAZIN, P. ELLEAUME, M. VELGHE, M. BILLARDON, Y. FARGE, J.M. ORTEGA, D.A.G. DEACON, J.M.J. MADEY, Y. PETROFF, K.E. ROBINSON	8. CONTRACT OR GRANT NUMBER(s) F49620-80-C-0068
9. PERFORMING ORGANIZATION NAME AND ADDRESS STANFORD UNIVERSITY STANFORD, CA 94305	10. PROGRAM ELEMENT, PROJECT, TASK AREA & WORK UNIT NUMBERS 61102F 2301/A1
11. CONTROLLING OFFICE NAME AND ADDRESS AFOSR/NP BOLLING AFB, DC 20332	12. REPORT DATE JUNE 1981 13. NUMBER OF PAGES 31
14. MONITORING AGENCY NAME & ADDRESS(if different from Controlling Office)	15. SECURITY CLASS. (of this report) UNCLASSIFIED 15a. DECLASSIFICATION/DOWNGRADING SCHEDULE

16. DISTRIBUTION STATEMENT (of this Report)

APPROVED FOR PUBLIC RELEASE; DISTRIBUTION UNLIMITED

17. DISTRIBUTION STATEMENT (of the abstract entered in Block 20, if different from Report)

18. SUPPLEMENTARY NOTES

Presented at the 1981 ONR Workshop on Free Electron Laser, Sun Valley

19. KEY WORDS (Continue on reverse side if necessary and identify by block number)

20. ABSTRACT (Continue on reverse side if necessary and identify by block number)

A superconducting undulator has been installed on the ACO storage ring and operated as a synchrotron radiation source, and as a free electron amplifier. We report measurements of the spontaneous emission spectrum, the gain as a function of the electron energy, and the laser induced lengthening of the electron bunch.

DD FORM 1 JAN 73 1473 EDITION OF 1 NOV 65 IS OBSOLETE

UNCLASSIFIED

SECURITY CLASSIFICATION OF THIS PAGE (When Date Entered)

RESULTS OF THE FIRST PHASE OF THE ACO STORAGE RING LASER EXPERIMENT

C. Bazin[1], M. Billardon[2], D.A.G.Deacon[3], P. Elleaume[4], Y. Farge[5], J.M.J. Madey[3], J.M. Ortega[2], Y. Petroff, K.E. Robinson[3], M. Velghe[6].

LURE, Bâtiment 209C, Université de Paris-Sud, 91 405, Orsay-FRANCE

1. Laboratoire de l'Accélérateur Linéaire, Bâtiment 200, Université de Paris-Sud 91405, Orsay, France.

2. Ecole Supérieure de Physique et de Chimie, 10 rue Vauquelin 75231 Paris Cedex, France.

3. Permanent address : High Energy Physics Lab, Stanford University, Stanford, CA, 94305, U.S.A.

4. Departement de Physico-Chimie, Service de Photophysique, C.E.N. Saclay, 91190 Gif-sur-Yvette, France.

5. Present address : D.G.R.S.T. 35, rue St Dominique, 75700 Paris, France.

6. Laboratoire de Photophysique Moléculaire, Bâtiment 210, Université de Paris-Sud, 91405, Orsay, France.

ABSTRACT

A Superconducting undulator has been installed on the ACO storage ring and operated as a synchrotron radiation source, and as a free electron amplifier. We report measurements of the spontaneous emission spectrum, the gain as a function of the electron energy, and the laser induced lengthening of the electron bunch.

INTRODUCTION

The possibility of operating a free electron laser in a storage ring has attracted a great deal of interest in recent years[1-9]. A collaboration has been established between LURE and Stanford to examine the initial experimental questions posed by the storage ring laser with the LURE undulator mounted on the storage ring ACO. The goals of the project have been to identify the characteristics of the emitted radiation with and without an external laser field, and to investigate the effects of the laser on the stored electron beam. We are at present constructing an optical klystron type undulator[10-11], which will increase the gain and should permit operation of the system as a laser oscillator. In this paper, we report on the measurements taken with the superconducting undulator[12].

The undulator has 23 periods of 4 cm wavelength, and is capable of producing up to 4.6 kG on the axis of the electron beam. A cross section of the vacuum chamber and the magnet poles is shown in figure 1. The storage ring is injected with the undulator in the up position so that the beam sees the large transverse aperture. After injection, the electron beam damps down to a small cross section, and the undulator can be lowered until the beam passes through the small finger of the vacuum chamber between the pole faces. The magnetic field can then be turned on, producing spontaneous radiation which leaves the vacuum chamber through a sapphire window.

The undulator is mounted on ACO as shown in figure 2. ACO is primarily used as a synchrotron radiation source, and operates without too much difficulty between the injection energy of 240 MeV and its maximum energy of 540 MeV. A current if 100 ma can be stored at these energies. However, in order to obtain emission in the visible with the present undulator, it is necessary to lower the operating energy to 150 MeV. Considerable difficulty has been encountered in retaining large currents at the low energy, as will be explained later. The currents obtained for the gain experiment represent a considerable success.

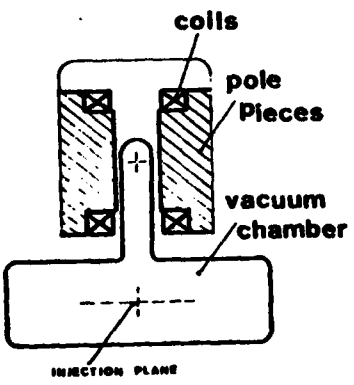

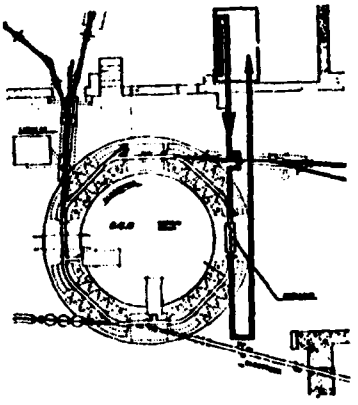

Fig. 1 - Cross section of the undulator vacuum chamber showing the disposition of the magnetic pole faces on each side of the beam position with the undulator lowered.

Fig. 2 - Location of undulator on ACO, and placement of experimental beam lines.

The low current bunch dimensions calculated for ACO at 150 MeV are σ_h = .21 mm and σ_v = .16 mm in the undulator straight section and the bunch length is σ_t = .87 nsec at V = 4kV and moderate coupling. Due to the low energy and the complex vacuum chamber geometry, each of these dimensions depends on the multiple Touschek effect[13] and the distribution of the trapped and partially swept positive ion distribution. The bunch length is also influenced by the anomalous bunch lengthening[14]. All dimensions have been observed to expand by factors of more than 3 for moderate current. Since the effects of the trapped ions and the bunch lengthening are not well characterized for the present ACO configuration, the dimensions must be measured under the conditions of the experiment.

Total useful experimental time has been limited by an anomalously low lifetime, and vacuum and cryogenic difficulties to about 30 hours on the spontaneous radiation, and a total of about 8 hours on the gain and the bunch lengthening. In May, after most of the technical difficulties had been worked out, the undulator developed an irreparable open circuit during the first bunch lenghthening run. Despite the technical problems, the present undulator has enabled us to obtain significant data on the spontaneous emission, its dependence on the beam alignment, the gain of the storage ring laser, and the laser induced beamheating. These results will be described in the following sections.

ELECTRON TRAJECTORY AND SPONTANEOUS EMISSION

Experimental studies indicate in a first approximation that most features of the spontaneous emission agree with theoretical predictions. However some disagreements from the theory of an ideal undulator are observed concerning for example a strong asymmetry of the coloured rings and a broadening of the spectral distribution. This arises from the fact that the mean electron trajectory is not a straight line. A first effect comes from a lateral displacement of the electron beam from the undulator axis, and can be eliminated if the electrons are injected on the magnetic axis with a velocity parallel to this axis[16]. For the results reported here, the alignment was good; the deviations from the ideal theory stem from an imperfect magnetic field.

In the superconducting undulator the magnetic field is not a perfect sinusoid. Edge effects modify the periodicity and intensity of the field at both ends of the undulator. Measurements of the magnetic field, along the $\hat{z}$ axis can be characterized by the expression :

$$\vec{B} = Bo\ H(z)\ \hat{y} \qquad (1)$$

(see Fig. 3 for definition of the system of axes).

In a perfect undulator $H(z) = \sin qz$, but experimentally it deviates from the pure sinusoidal form with :

$$H(z) = 1 \pm 5\% \qquad q = \bar{q} \pm 3\% \qquad \int_0^L H(z)\,dz = 0$$

In order to determine the effets of this deviation we have calculated the electron trajectory and the emission spectra using the experimental H(z) function[17] with the initial conditions y = 0 and $\beta_y = 0$. The trajectory remains in the xz plane and the equations of motion are given by :

$$\beta_x(Z) = \beta_0 - (K\bar{q}/\gamma)\int_0^z H(z')\,dz' \qquad \beta_z = 1 - \frac{1}{2\gamma^2} - \frac{\beta_x^2}{2} \qquad (2)$$

$$x(z) = \beta_o z - (K\bar{q}/\gamma)\iint H(z')\,dz'$$

where β_o is the initial velocity along the x axis, $\bar{q}$ is the mean period of the undulator and $K = eB_o/mc^2q$ is given by the amplitude B_o of equation (1).

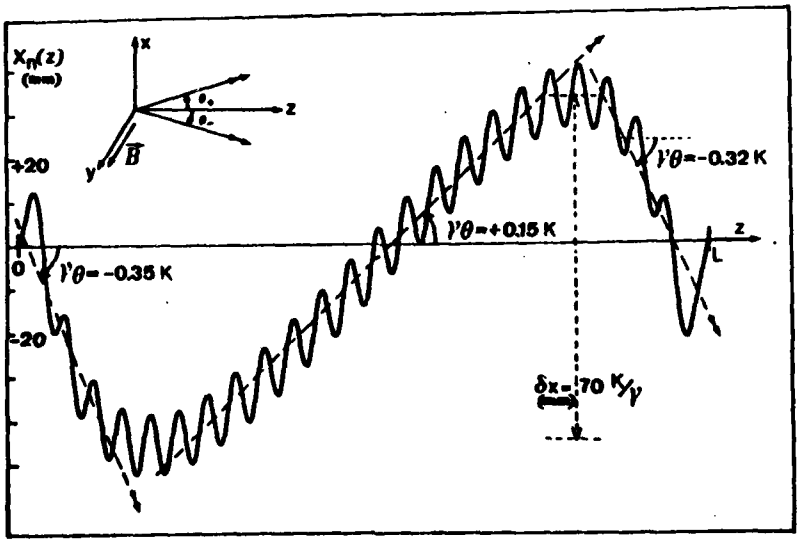

Fig.3 - Calculated electron trajectory in the xz plane. The undulator has 23 periods and a length L = 960 mm. The value of the x component of the trajectory is given by : $x(z) = (K/\gamma)\, X_n(z)$

Therefore, the motion is defined by the integrals of the field and the initial velocity. In the most usual case β_0 is chosen so that the mean trajectory is parallel to the magnetic field $\hat{z}$ axis defined by $x(0) = 0$ and $x(L) = 0$ and Fig.3 shows the calculated trajectory $s(z)$ for our 23 period undulator. If the undulator was perfect the mean trajectory would be along the z axis, but in the actual case it is a winding path. The inner-most part of the trajectory is tilted with an angle of $\gamma\theta \simeq +0.15K$, whereas at each end the trajectory bends in the other direction with $\gamma\theta \simeq -.35K$. Schematically we would obtain the same result with a series of three tilted undulators; an observer sees the successive periods of the trajectory at different angles. For example, in the direction of the central section $\gamma\theta = .15K$, about 17 periods emit on the same wave length. A red shifted emission is produced by the other sections according to the law $\lambda = \lambda_o/2\gamma^2 \times (1 + K^2/2 + \gamma^2\theta^2)$. The inference of the radiation of the three sections of the undulator produces a radiation spectrum whose width and shape depend strongly on the angle of observation. The broadening of the spectrum reduces the gain by a factor which approaches 50%. In the mean direction $\gamma\theta = (+0.15K-0.35K)/2$, all periods are observed from the same angle. For this particular direction only, features of the perfect undulator are obtained.

An exact numerical calculation of the emission can be performed using the equations of motion (2) and the classical formula[18] :

$$\frac{dw}{d\Omega d\omega} = \frac{e^2\omega^2}{4\pi^2 c}\left[\int_o^T \hat{n} \times (\hat{n} \times \vec{\beta}) \exp(i\omega(t - \hat{n}.r/c)\, dt\right]^2 \qquad (3)$$

The result is given by :

$$\frac{dw}{d\Omega d\omega} = \frac{e^2}{c}\,\frac{(\bar{q})^2}{2\pi}\,\frac{\gamma^2}{(1+K^2/2)^2}\,S(\rho) \qquad (4)$$

where $S(\rho)$ is the spectrum profile and ρ the normalised frequency

$$\rho = \frac{\omega}{\omega_{\theta=0}} = \omega\,\frac{(1+K^2/2)}{\bar{q}c\ 2\gamma^2} \qquad (5)$$

Fig. 4 shows the calculated spectra obtained for K = 1.8 and three $\gamma\theta$ directions in the xz plane. The most important features are summarized below.

1) The classical $\sin^2 x/x^2$ profile is no longer present. The shape of the spectrum is strongly dependent on θ. For $\gamma\theta << 0$, there are no secondary maximas on the low-frequency side whereas the maxima on the high frequency side are greatly enhanced. For $\gamma\theta >> 0$ an inverse situation is obtained, but the secondary maxima are not as large. The profile of the main peak also exhibits an asymmetry which is θ dependent.

2) A strong variation of the width of the central peak is observed. For our undulator the relative width is maximum ($\lambda/d\lambda = 17$) in the direction of the center of the coloured rings of the spontaneous emission ($\gamma\theta = +0.25$) whereas a value of $\lambda/d\lambda = 25.5$ is obtained for $\theta \simeq 0$. This last value is very close to the theoretical one ($\lambda/d\lambda = 26$).

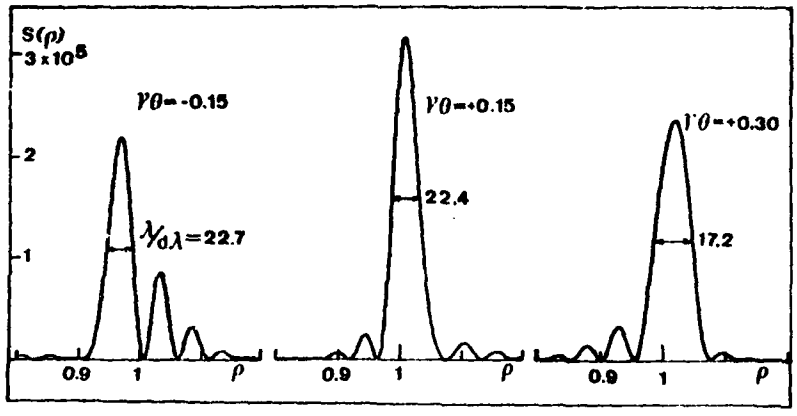

Fig. 4 - Spectral distribution of the spontaneous emission as a function of the normalised frequency $\rho = \omega/\omega(\tau=0)$ calculated for K = 1.8 and three directions of observation in the xz plane. The origin $\theta = 0$ corresponds to the magnetic field z axis; $\gamma\theta \simeq 0.25$ is approximately the angle of the center of the ring system.

3) The maximum spontaneous intensity, the minimum spectralwidth, the minimum central wavelength and the maximum gain are each obtained in different directions. With K = 1.8 we have :

I max : $\gamma\theta \simeq 0.05$
$d\lambda$ min : $\gamma\theta \simeq 0$
λ min : $\gamma\theta \simeq 0.25$ (center of the rings)
G max : $\gamma\theta \simeq 0.05$

4) For the FEL, the optical gain is related to the derivative of the spectral distribution. Fig.5 shows the calculated gain for $\gamma\theta$ = .10 and .30; the direction $\gamma\theta$ = .30 is close to the center of the rings, so that the right hand curve can be compared with

the measured gain curve presented in the next section.

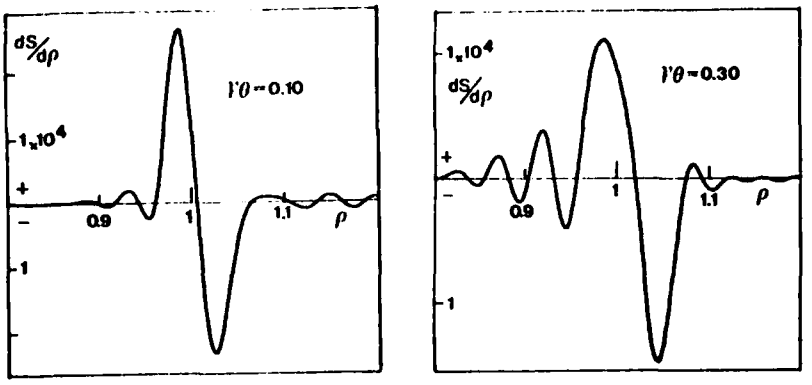

Fig. 5 - Spectral distribution of the gain calculated from the derivative of the spontaneous emission.

Measurements have been made of the spectral distribution versus the θ angle in the xz plane. The optical apparatus is shown schematically in Fig. 6. A 75μ pinhole is set in the focal plane of the M_1 mirror, so that all the radiation emitted at a given angle in the undulator is collected at that point with a resolution of $\delta\theta = 4.10^{-5}$ rad. Fig. 7 shows the spectra obtained for three directions θ' defined with respect to the center of the spontaneous ring system. Qualitatively, all effects described above are observed. Some small differences are observed between the experimental results and the calculated ones. Probably this discrepancy is due to the fact that the H(z) function was measured for weak fields, while for the emission experiments we used a larger field close to the maximum obtainable with the undulator. The geometry of the field could be slightly

different due to saturation effects so that the actual trajectory was not exactly the same as the one shown on Fig. 3.

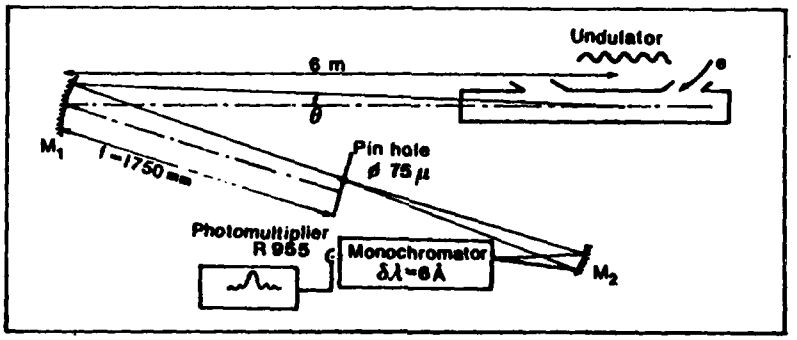

Fig. 6 - Optical setup for angular and spectral distribution studies.

Experimentally the relative width varies from 17.5 to 23 and the theoretical value was not reached in any direction. This residual broadening is due to the emittance of the electron beam. The minimum of the spectral width is obtained for $\gamma\theta' \simeq -0.30$, a direction which is very different of the ring center. According to the law $\lambda = (\lambda_o/2\gamma^2) \times (1 + K^2/2 + \gamma^2\theta^2)$, the dispersion of the velocity in the bunch now contributes in a linear fashion to the inhomogeneous broadening so that $\lambda/d\lambda = 23$ is the largest value observed.

Taking into account the actual electron trajectory, theoretical and experimental features of the spontaneous emission are in very good agreement. The magnitude of these effects demonstrate the very high sensitivity of the emission to small deformations of

the mean trajectory or equivalently, to small differences between the actual magnetic field and the sinusoidal one. It is interesting to note that such deviations have also been observed in the infra-red Stanford experiments using a helical undulator (see Fig. 2 of Ref. 19). The best Stanford spectra exhibit broadening stronger than can be explained by energy spread and emittance effects, and show pronounced asymmetry of the secondary maxima. Since it is known that the helical magnet exhibits some deviation from a straight line, it is likely that magnetic field errors are responsible for these deviations in the form of the spectrum.

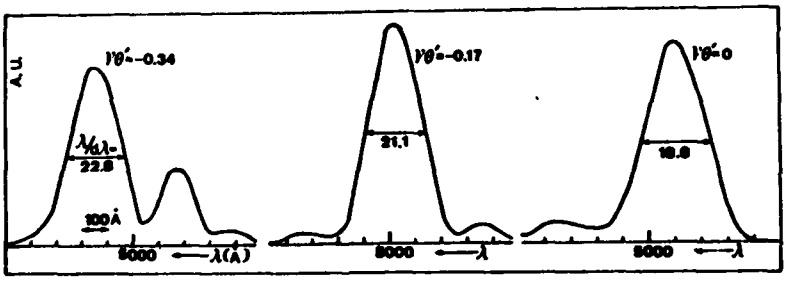

Fig. 7 - Experimental spectra measured for K = 1.5 and E = 150 MeV. Here, the origin θ' = 0 corresponds to the ring center.

GAIN MEASUREMENT

We have obtained measurements of the gain as a function of energy at two wavelengths in the visible, 5145Å, and 4880Å, and for several different magnetic fields. As the gain is very low, the average gain being on the order of 10^{-6}, a double demodulation

technique with a noise level equivalent to a mean gain of 10^{-8} has been employed [20]. As shown in Fig. 8, a CW argon laser is focussed to a waist at the center of the undulator, and the laser beam is adjusted to travel coaxially with the electron beam. The laser is amplified at the frequency of the electron beam, 27.2 MHz, and the signal is obtained by a detector resonant at this frequency, after which it is demodulated. The laser is chopped at low frequency to permit subtraction of the spontaneous emission signal, and the gain is extracted in a second lock-in slaved to the chopper. The collimation and the passage of the beam through the monochromator reduce the spontaneous power incident on the detector.

Calibration is performed with the synchrotron radiation emitted in the fringing field of one of the main dipole magnets ateach end of the undulator straight section. This beam is chopped to produce a beam with the same time structure as the gain, and a signal V^o_{RF} is observed through the detection system. At the same time, the total power incident on the diode is monitored at a port on the detector which bypasses the resonant filter; this signal, which can be observed on a low frequency lock-in, is measured as V^o_{LF}. Under the conditions of the experiment, a small signal V_{RF} is measured, which corresponds to a total amplified power in the LF port of $(V_{RF}/V^o_{RF})V^o_{LF}$. The signal actually measured in the LF port is dominated by the chopped laser power V_{LF}. The average gain $\bar{G}$ produced in the inter-

action is then the ratio between the total amplified power and the total incident power

$$\bar{G} = \frac{V_{RF}}{V_{RF}^{o}} \quad \frac{V_{LF}^{o}}{V_{LF}} \qquad (6)$$

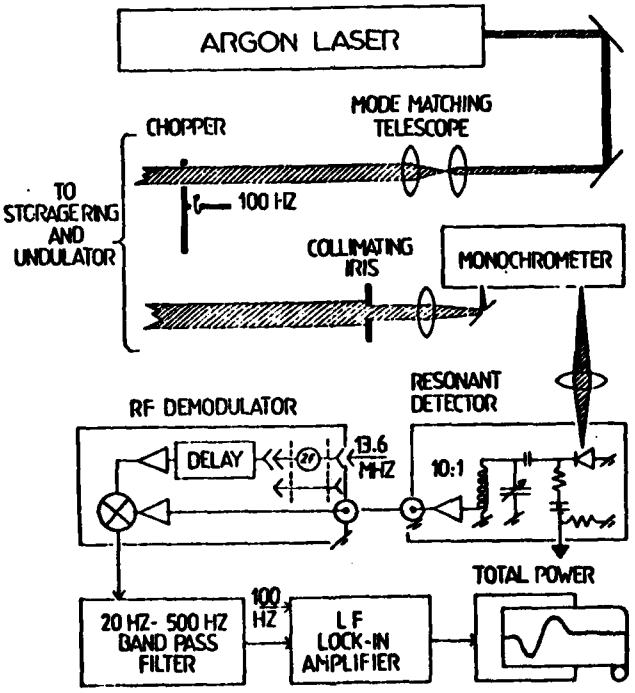

Fig. 8 - Schematic diagram of the gain experiment, showing beam transport and signal processing systems.

The anticipated gain can be calculated for a linear undulator from the fourth component of the Lorentz force equation.

$$\frac{d\gamma}{dt} = \frac{e}{mc^2}\vec{E}\cdot\vec{v} \simeq \frac{e}{mc}\frac{EK}{\gamma}\cos(kz-\omega t)\cos qz \qquad (7)$$

along the lines of Colson's original calculation for a helical undulator[21]. The equation is recast using $z(t)$ as independent variable, the resonant terms are identified using a Bessel function expansion, and the equation is integrated in perturbation expansion to second order. The gain is obtained by integrating the energy loss over the electron distribution in transverse positions, angles, energy, and optical phase, and by dividing by the energy density in the optical field.

$$G_{linear} = G_{helical}\frac{1}{2}\left[J_{\frac{n-1}{2}}(\xi) - J_{\frac{n+1}{2}}(\xi)\right]^2 \frac{1}{\sqrt{(1+\frac{w_o^2}{4\sigma_h^2})(1+\frac{w_o^2}{4\sigma_v^2})}} \qquad (8)$$

where

$$G_{helical} = \rho r_o \lambda_o^2 \frac{16\pi^2 nK^2N^3}{\gamma^3}\left(\frac{1-\cos x-\frac{x}{2}\sin x}{x^3}\right) \qquad (9)$$

for a perfect undulator $H(z) = \sin qz$ and small inhomogeneous broadening.

In these equations n is the harmonic number of the on-axis radiation (n is odd), $\xi = nK^2/(4+2K^2)$, w_o is the beam waist of the optical mode and σ_h and σ_v are the root mean square horizontal and vertical electron beam dimensions. The peak electron density is ρ, $r_o = e^2/mc^2$, and the detuning pa-

rameter is $x = 4\pi nN\delta\gamma/\gamma$ where $\delta\gamma$ is the normalized energy deviation from the resonance energy. The filling factor has been calculated assuming coaxial beams and a Gaussian transverse electron distribution.

In an undulator with an imperfect magnetic field, the x dependence of the gain must be modified. By virtue of Madey's theorem[22], this factor can be replaced by the derivative of the measured spontaneous power spectrum. Since the spontaneous measurement has no absolute calibration, this technique provides only the shape of the gain curve. To find the amplitude, we have calculated the reduction in the gain produced by the measured magnetic field distribution as discussed in the previous section. If we identify the unknown angle of observation in the calculation by requiring that the width of the spontaneous curve agree with the measured value, the calculation then predicts a reduction in the gain by a factor .39 from the level (8). The effects of the energy spread and beam emittance in the experiment are small compared to these trajectory effects, and have therefore been neglected. In the general case, the filling factor must also include the misalignment of the mean axes of the two beams, and the mean transverse motion of the electron beam (Fig. 3) which has an amplitude of approximately $w_o/3$ in our experiment.

A plot of the gain measured as a function of energy is provided as figure 9. A spontaneous emission curve obtained under the same conditions after the previous injection is presented underneath for comparision. The small apparent energy shift is not significant due to the hysteresis present in the bending magnets of ACO which are cycled between injec-

tions. The extent of the energy sweep was limited both by the lifetime (8 min.) and by a beam instability which became bothersome on the low energy side of the data.

The spontaneous emission curve agrees well with the results of the calculations made from the low field undulator measurements and described in the previous section. Since the alignment technique used the highest frequency portion of the spontaneous emission beam as a reference axis, the approximate angle of observation is known. At this angle ($\theta' = 0$), the heights of the gain and absorption peaks are about equal, but depend strongly on the observation angle, and the curve is broadened by a factor of about 1.4.

Experimentaly, the baseline of the gain curve is undetermined. However, its position can be estimated from the fact that the gain is related to the derivative of the spontaneous emission curve[22]. As shown in the figure, the absorption peak drops monotonically to zero on the low energy side, and a secondary absorption peak is evident on the high energy side. Although this behaviour is qualitatively correct, there remains some uncertainty on the position of the baseline, and therefore on the value of the gain.

The peak gain measured during the run shown in figure 9 was 3×10^{-4} per pass. Other measurements yield gains both smaller and somewhat larger than this value. The short beam lifetime did not permit the execution of the final alignment of the laser on the electron beam. The preliminary alignment technique produces parallel beams with an unknown transverse displacement of the order of the electron beam dimension. The values of the gain measured therefore include a fluctuating filling factor, and represent lower bounds for the gain of a well centered beam. Due to the good agreement of the theoretical and the measured results,

the alignment is believed to be good for the results shown.

The predominant uncertainties in a calculation of the theoretical gain for the case of figure 9 come from the factors which enter into the current density. Due to the absence of good diagnostics for the bunch dimensions and the stored current in ACO, these quantities are known with an accuracy of at best 25% with an added uncertainty in the bunch dimensions due to the imperfect data on the machine optics. The calculated value of $\bar{G}$ carries a smaller error bar because of the absence of the bunch length. The theoretical value of $\bar{G} = 4.1 \begin{smallmatrix} + 1.5 \\ - 2.2 \end{smallmatrix} \times 10^{-6}$ is the same as the measured value of $(6.5 \pm 1.6) \times 10^{-6}$ within the uncertainties.

A similar experiment has been performed at Novosibirsk[23] using an optical klystron installed on the storage ring VEPP-3. Although absolute measurements of the gain have not been carried out, the dependence of the gain on the energy and its order of magnitude at 6328 Å have been shown to agree with the theory. One interesting technique used in this experiment is polarization modulation of the laser. This technique eliminates the feed-through of the spontaneous emission in the gain measurement caused by impedance modulation of the diode detector[20].

Future experiments at Orsay will be performed with the undulator/optical klystron now under construction. In particular, we plan to investigate the dependence of the gain on the filling factor by varying the alignment of the laser. The development of improved diagnostics on the electron beam will also allow a more precise comparision of the gain with the theory.

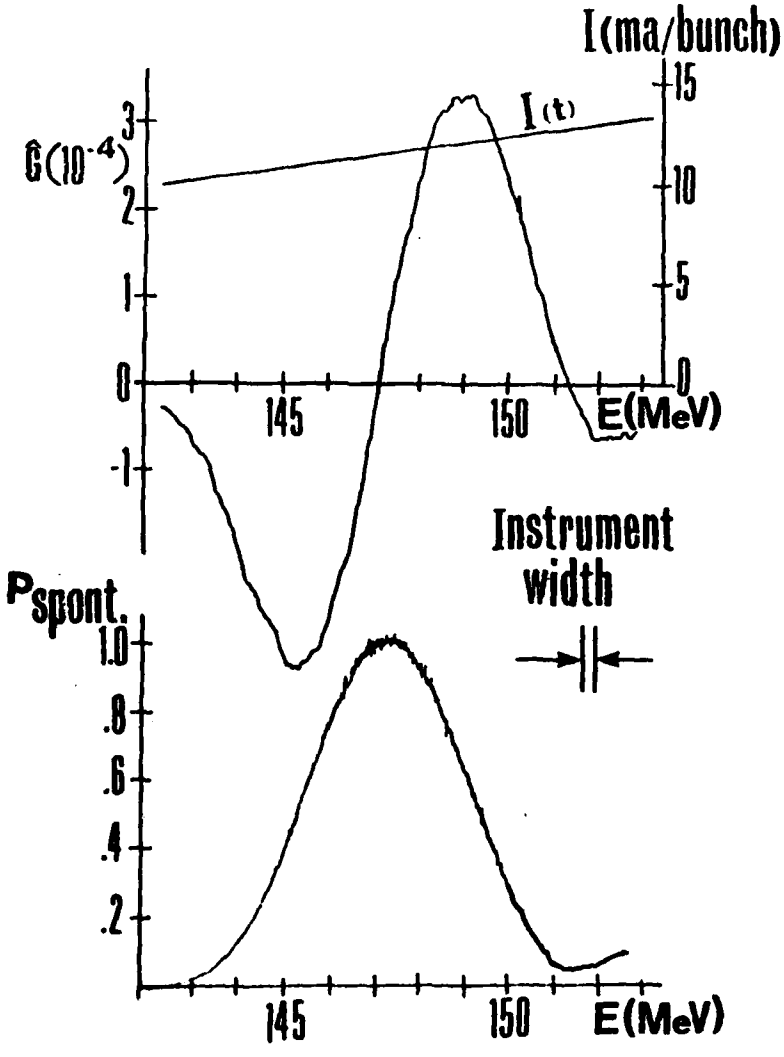

Fig. 9 - Gain and spontaneous emission spectra measured for the ACO superconducting undulator, with λ = 4880 A° and K = 1.5. The estimated bunch dimensions and average current are σ_h = .26 mm; σ_v = .15 mm; σ_T = .29 nsec, and I = 12 ma per bunch, all of which are known to an accuracy of approximately 25%. The average and peak gains at 149 MeV are $\bar{G}$ = $(6.5 \pm 1.6) \times 10^{-6}$ and $\hat{G}$ = $(3.3 \pm 1.2) \times 10^{-4}$ where $\bar{G}$ has the larger relative error due to the uncertainty of the bunch length.

BENCH LENGTHENING MEASUREMENT

The first order effect of the free electron laser interaction is an energy modulation induced on the electron beam with period equal to the optical wavelength. This effect is very important in storage ring lasers where the additional energy spread can accumulate on the electron beam from pass to pass. The resultant increase in the bunch length contributes to the saturation of the gain; for low gain systems such as ACO, it can be the dominant effect.

The root mean square energy modulation induced per pass in the laser can be calculated by integrating (7) to first order.

In the stochastic phase approximation, an electron's optical phase is uncorrelated from pass to pass, and the mean square energy spread per pass of the beam is calculated by averaging over the initial phase and the electron distribution as before.

$$\overline{\left(\frac{\delta\gamma}{\gamma}\right)^2} = \frac{Ir_o\lambda^2}{mc^3}\,\frac{\pi K^2 N^2}{\gamma^4}\left[J_{\frac{n-1}{2}}(\xi) - J_{\frac{n+1}{2}}(\xi)\right]^2 \frac{\left(\frac{\sin x/2}{x/2}\right)^2}{\sqrt{\left(\frac{4\sigma_h^2}{w_o^2}+1\right)\left(\frac{4\sigma_v^2}{w_o^2}+1\right)}} \qquad (10)$$

For the imperfect undulator used on ACO the spectral dependence of the laser induced heating follows from the result first demonstrated by Madey that the mean squared energy spread is proportional to the spontaneous power spectrum[22]. The modification to (10) which stem from the field imperfections are calculated from the measured magnetic field distribution as was done for the gain in the previous section.

If the laser does not modify the damping times of the electron beam [3-7], it follows from the stochastic phase approximation that the equilibrium energy spread of the stored beam in the presence of the laser heating is:

$$\left(\frac{\sigma_e}{E}\right)^2 = \left(\frac{\sigma_e}{E}\right)_o^2 + \frac{\tau}{4T_o}\left(\frac{\delta\gamma}{\gamma}\right)^2 \qquad (11)$$

for low current, where $(\sigma_e/E)_o$ is the natural low current energy spread,[24] τ is the energy damping time, and T_o is the revolution period (for ACO, T_o = 73.4 nsec). The bunch length is related to the energy spread through:

$$\sigma^2 = \frac{\alpha^2}{\Omega^2}\left(\frac{\sigma_e}{E}\right)^2 \qquad (12)$$

where α is the momentum compaction factor, and Ω is the angular synchrotron frequency[24]. For large currents, additional terms appear in equation (11) and (12) due to such factors as the multiple Touschek effect[13], and anomalous bunch lengthening . The analysis of the effect of the laser at higher currents is complicated by the fact that these additional terms depend on the current density, and therefore indirectly on the laser heating.

An experiment has been assembled on ACO to measure the bunch lengthening induced by the laser on the electron beam In this section, we describe the experiment and the preliminary measurements taken before the demise of the superconducting undulator.

Synchrotron light is emitted by a storage ring in a series of pulses separated on the average by T/m where m is the number of bunches stored. In the frequency domain, this produces a comb spectrum multiplied by the transform of the charge density as a function of time in a single bunch.

In this experiment, two bunches were stored so that the fundamental frequency was 27.2 MHz, with a small signal present at harmonics of half this frequency due to differences in the two bunches. Any given harmonic will have an amplitude which is directly related to the length of the bunches. A measurement of the change of this amplitude yields the change in the bunch length, while a measurement of the envelope function yields the bunch length itself.

If we model the bunch as a Gaussian with standard deviation σ, the amplitude of the frequency spectrum of the synchrotron light at the harmonic frequency ω is proportional to:.

$$F(\omega) \sim P(\omega) e^{-\sigma^2\omega^2/2} \qquad (13)$$

where $P(\omega)$ is the transform of the time response of the measurement system to the passage of a single electron in the ring. A change in σ is related to a change in the harmonic amplitude through:

$$\Delta\sigma^2 = -\frac{2}{\omega^2} \ln \frac{F_i(\omega)}{F_f(\omega)} \qquad (14)$$

where we have defined $\Delta\sigma^2 = \sigma_f^2 - \sigma_i^2$.
The response time of the measuring system drops out entirely. $P(\omega)$ does, however, need to be measured in order to extract the bunch length σ from the measured $F(\omega)$.

The change in the square of the bunch length, $\Delta\sigma^2$, is related directly to the heating so long as equations (11) and (12) remain valid:

$$\Delta\sigma^2 = \frac{\alpha^2}{\Omega^2} \frac{\tau}{4T_o} \left(\frac{\delta\gamma}{\gamma}\right)^2 \qquad (15)$$

The fractional change in the bunch-length $(\delta\sigma/\sigma_i)$ can be calculated once σ_i is known.

$$\delta\sigma/\sigma_i = \sqrt{\Delta\sigma^2/\sigma_i^2+1} - 1 \qquad (16)$$

A schematic of the experimental apparatus is provided as figure 10. The synchrotron light is detected by an RTC TVHC40 vacuum photodiode with a response time measured with a 7 picosecond dye laser to be (980 ± 10) psec FWHM. A spectrum analyser provides the information for the bunch length measurement in the scanning mode: changes in σ are measured at fixed frequency and bandwidth.

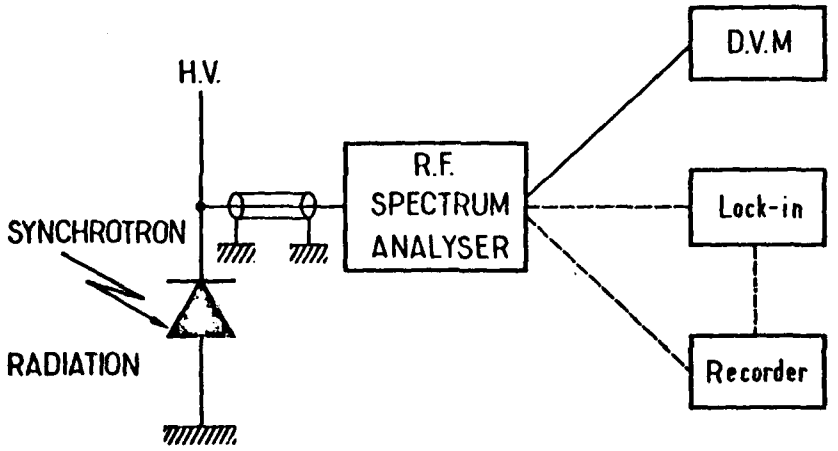

Fig. 10 - Simplified schematic of bunch lengthening experiment.

The choice of the harmonic at which the measurement of the bunch lengthening is to be made is extremely important. The relative amplitude change increases as the square of the frequency for a given change in the bunch length, but at the same time the signal drops into the noise.

Since the electron beam radiates noise directly into a large number of harmonics, and a portion of this radiation

is coupled into the measurement system, the operating point must be selected with the aid of a measurement of the harmonic pickup. Low frequency noise is produced by the coherent oscillations between the stored bunches and within each bunch. The inter-bunch oscillations (phase oscillations) produce sidebands on each harmonic. The measurement is made insensitive to these oscillations by choosing the detection bandwidth sufficiently large (100 kHz in the experiment). Oscillations of the charge density within the bunch, however, produce fluctuations in the envelope of the spectrum, and act as a noise source dependent on the RF voltage, the current density and the energy.

The experiment has been designed to operate with a synchronous detector in order to increase the sensitivity. The laser can be chopped at a speed limited by the damping time of the energy oscillations in the ring (τ = 240 msec at 156 MeV); the change in the bunch length is extracted from the noise in a lock-in. The instrumental limitation on the sensitivity to $\Delta F/F$ has been measured at 10^{-8} in this configuration. In any experiment, the limiting sensitivity is likely to be set by the noise sources internal to the electron beam.

Figure 11 shows the measurements of the bunch lengthening observed on ACO at 156 MeV with a field of 4.6 kG in the superconducting undulator, and the argon laser operating at 5145 A°. The relative change in the harmonic amplitude at $\omega_o = 2\pi(654\ \text{MHz})$ is shown as a function of the laser power at the electron beam.

Using equation (16) and the measured value $\sigma = 270 \pm 30$ psec the relative change in the bunch length can be obtained from $\Delta F/F$ by multiplying by $.9 \pm .2$. The maximum bunch lengthening observed was (3.7 ± 1.0) % at the laser intensity $I = (220 \pm 80)\ \text{w/cm}^2$. The dependence on the intensity is linear

as expected from equation (11) for small changes in the energy spread.

The vertical polarization vector of the laser light at the entrance to the vacuum chamber is modified by its passage through the sapphire window. Due to a machinist's error, this window was placed with its birefringent axis at 17.5° to the vertical so that the vertical polarization component of the transmitted beam was reduced in intensity by an unknown factor whose magnitude lies between 0.67 and 1.0. Since only the vertical component of the polarization interacts with the beam, the bunch lengthening is reduced by this factor. (Note that the polarization rotation was present only for the set of runs during which the bunch lengthening measurements were performed).

An independent reduction of the bunch lengthening effect is produced by residual alignment errors.The initial alignment proceedure produces parallel beams with a transverse separation on the order of the beam dimension. Under favorable conditions, the alignment can be optimized on either the magnitude of the gain, or the bunch lengthening. During this run, however, the gain was too small to be seen due to the low current, and a storage ring malfunction intervened before the noise on the bunch lengthening signal could be reduced sufficiently for the bunch lengthening itself to be used for this purpose. The measured value of the bunch lengthening is therefore a lower bound on that which would be produced with vertical polarization and aligned beams.

The theoretical value for the bunch lengthening expected for a well aligned system can be obtained from equations (10) and (11). Using the best available values for the bunch dimensions, and including the effects of the real

magnetic field and the polarization rotation, the fractional increase in the bunch length is calculated to be 13%-20%. A misalignment of 0.6-0.7 mm would be needed to explain the difference between the observed and theoretical values.

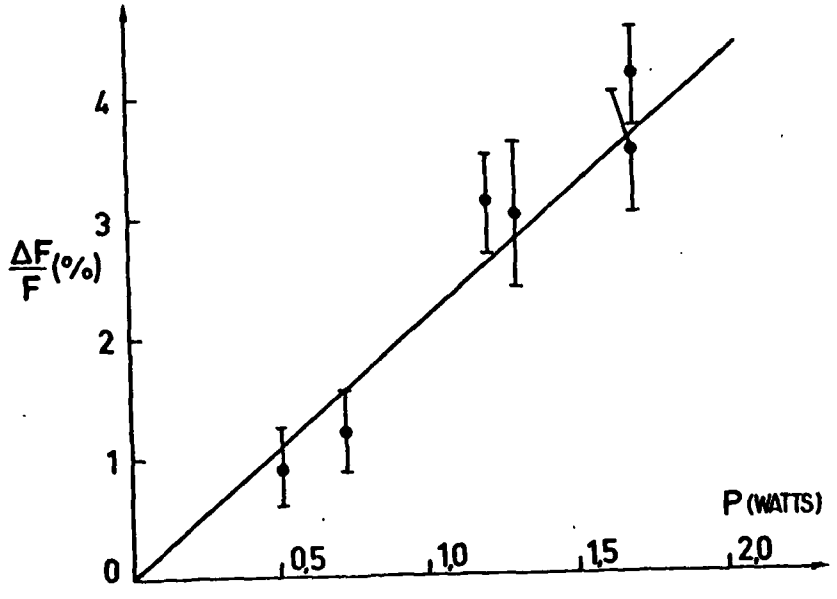

Fig. 11 - Relative change in the harmonic amplitude measured as a function of laser power. To obtain $\delta\sigma/\sigma$ vs. laser intensity multiply the vertical axis by $(.9 \pm .2)$ and the horizontal axis by (130 ± 50) cm^{-2}. The bunch length was measured to be $\sigma = (270 \pm 30)$ psec, the harmonic frequency was $\omega_0 = 2\pi(654\ MHz)$, the laser beam waist was $w_0 = 6mm$, and the transverse electron beam dimensions were $\sigma_h = .2 \begin{matrix} + .2 \\ - .0.5 \end{matrix}$ mm and $\sigma_v + 0.3 \begin{matrix} + .3 \\ - .08 \end{matrix}$ mm

Since the alignment tolerance was $\pm$.5mm, it is apparent that the measurement is consistent with the theory. Our measurements prove the existence of the laser induced bunch lenghening effect, and verify that the size of the effect is in rough agreement with the theory.

The present work has been severely handicapped by a number of problems encountered with the superconducting undulator and ACO. While the initial sensitivity to the head-tail effect[25] at low energy was substantially improved after we installed a set of manually controlled sextupoles to annul the chromaticity of the ring, severe current loss was sustained during the descent in energy and the lowering of the of the undulator. These losses appear to be unavoidable for low energy operation, as they stem from trapped ion instabilities and harmonic radio-frequency beam excitation due to the form of the vacuum chamber in the undulator, respectively. The latter effect may also be responsible for the anomalously low lifetime (τ=8-30 min) observed with the undulator down. The gain measurement, in particular, being sensitive to the current density, was extremely difficult to obtain.

The new optical klystron has been designed to eliminate the worst of these problems. The radiofrequency excitations, the current losses in lowering the energy and the undulator, and the low lifetime should be much improved by the larger, fixed vacuum chamber and the new magnet wavelength which will permit operation in the visible at the injection energy. The technical problems associated with a bakeable superconducting system are eliminated through the choice of permanent magnets. In addition, the anomalous spectral dependence due to the twisted nature of the orbits in the

present undulator will be eliminated. Once the electron beam current and dimensions are characterized at the operating energy, progress is expected to be much more rapid with the new system and the higher gain should allow examination of the laser properties in the threshold region.

This work has been supported by :
the D.G.R.S.T., contract 79-7-0163,
the D.R.E.T., contract 9-073,
and the A.F.O.S.R., contract F 49620-80-C-0068.

REFERENCES

1. L.R. Elias, W.M. Fairbank, J.M.J. Madey, H.A. Schwettman, T.I. Smith; " A discussion of the potential of the free electron laser as a high power tuneable source of infrared, visible, and ultraviolet radiation"; published in Proceedings of the Synchrotron Radiation Facilities Summer Workshop. University Laval, Québec, Canada, June 1976.
2. J.M.J. Madey and D.A.G. Deacon. "Free Electron Lasers", published in Cooperative Effets in Matter and Radiation, Bowden, Howgate & Robl (eds), Plenum, New-York, 1977.
3. N.A. Vinokurov, A.N. Skrinskii, "Limiting Power of an Optical Klystron installed on an Electron Storage Ring", unpublished, INP 77-67 (1977). Institute of Nuclear Physics, 650090, Novosibirsk, USSR.
4. A. Renieri, Il Nuovo Cimento 53B, 160, (1979).
5. D.A.G. Deacon, J.M.J. Madey, Applied Physics, 19, 295 (1979)
6. J.M.J. Madey, D.A.G. Deacon, T.I. Smith, J. Appl. Phys. 50 7875 (1979).
7. L.R. Elias, J.M.J. Madey, T.I. Smith, Appl. Phys., 23, 273 (1980).
8. G. Dattoli, A. Renieri, Il. Nuovo Cimento, 59B, 1, (1980).
9. D.A.G. Deacon, J.M.J. Madey, Phys. Rev. Lett. 44, 449, (1980).
10. N.A. Vinokurov and A.N. Skrinskii, Preprint INP 77-59, Novosibirsk (1977) see also N.A. Vinokurov, Proc Xth Intl. Cong. on High Energy Charge Particle Accelerators, Serpukhov, vol. 2, 454 (1977).
11. P. Elleaume, "Optical Klystron Spontaneous Emission and Gain", elsewhere in this volume.
12. C. Bazin, Y. Farge, M. Lemonnier, J. Perot, Y. Petroff, Nucl. Inst. & Meth., 172, 61 (1980).
13. H. Bruck. Accélérateurs Circulaires de Particules, Presses Universitaires de France (1966), chap. XXXI, English

translation LA-TR-70-10 available from LASL, Los Alamos, New Mexico, 87544.

14. G.A. Voss, in Proceedings of the "Ettore Majorana" International School of Particle Accelerators, Blewett, M.M. (ed) Erice, 1976.
15. C. Bazin, M. Billardon, D.A.G. Deacon, Y. Farge, J.M. Ortega, P. Perot, Y. Petroff, M. Velghe, Journal de Phys. Lett. 41 (1980) 547.
16. B. Moussalam et al.,manuscript in preparation.
17. M. Billardon et al.,manuscript in preparation.
18. J.D. Jackson, Classical Electrodynamics, J. Wiley and sons, 1975, P. 671.
19. D.A.G. Deacon, L.R. Elias, J.M.J. Madey, G.J. Ramian, H.A. Schwettman and T.I. Smith, Phys. Rev. Let. 38, 892 (1977).
20. D.A.G. Deacon, J.M.J. Madey; K.E. Robinson; C. Bazin, M. Billardon, P. Elleaume; Y. Farge, J.M. Ortega, Y. Petroff, M.F. Velghe, I.E.E.E. Trans. Nucl. Sci., NS-28, 3142, (1981).
21. W.B. Colson, Phys. Lett., 64A, 190 (1977).
22. J.M.J. Madey, 11 Nuovo Cimento, 50B, 64 (1979).
23. G.A. Kornyukhin, G.N. Kulipanov, U.N. Litvinenko, N.A. Mezentsev, A.N. Skrinskii, N.A. Vinokurov, P.D. Voblyi, "The Experiments with an Optical Klystron installed on the VEPP-3 Storage Ring", Institute of Nuclear Physics, 630090, Novosibirsk, USSR.
24. M. Sands, "The Physics of Electron Storage Rings" : an Introduction", SLAC report No. 121 (1965), Stanford Linear Accelerator Center, Stanford, CA 94305.
25. M. Sands, "The Head-Tail Effect : An Instability Mechanism on Storage Rings", SLAC-TN-69-8, Stanford Linear Accelerator Center, Stanford, CA, 94305.

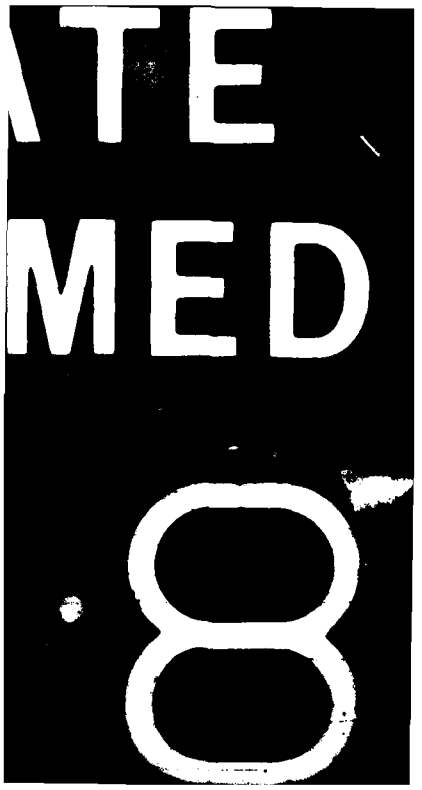
TE
MED
8